Testing and Isolation Efficacy; Insights from a Simple Epidemic Model

November 23, 2020

1 Abstract

2 Introduction

One of the main challenges in interpreting COVID-19 dynamics is to unravel/investigate information gained from data. The daily case count is a highly accessible form of data where observations are driven by two clusters of processes: (i) epidemic processes and (ii) testing processes. The challenge is then to separate these processes and understand how they interact. Simple mathematical models have a long history in providing useful insights facing with real epidemiological challenges (Ross, 1911) [maybe add influenza work, ideas?]. We developed a model that incorporates mechanistic processes of epidemic processes and testing. We used the model to study the potential effect of testing strategies and slow-fast reporting testing result.

There are different testing strategies with different test-specific efficacy, the time required for the results to be reported and the cost of the test. Testing strategies can be grouped into two broad categories including (i) random testing across the whole population and (ii) Non-random testing. Note that contact tracing is an example of non-random testing strategies. Each of these strategies has been used as a tool to study COVID-19; see (refs) for group (i) and (refs) for group (ii). The advantage of non-random testing comparing to random testing has been investigated specifically during the COVID-19 pandemic (refs).

Much effort has been invested in developing widely accessible and fast tests in order to mitigate the spread of the pandemic (refs). In order to have a sense and as a comparison of slow versus fast test, we provide an example. The viral PCR test, which is the most commonly used test and takes about four days, is very slow relative to the potential tests such as breath-based test (Ruszkiewicz et al., 2020), which is still in trial stage and takes a few seconds. The point to be made is that there can be a potential advantage of slow test.

In this work we developed a model to incorporate epidemic processes and testing processes mechanistically to study the potential effect of testing strategies and slow-fast testing. The analysis of the deterministic model included

deriving the basic reproduction number, $\mathcal{R}_0$, as the index of threshold dynamics and the effect of underlying parameters on this key index. We found that the non-random testing strategy is more effective than the random testing. Specifically, the required critical testing intensity to keep $\mathcal{R}_0$ lower than the threshold value of one is much lower in the non-random testing than the random one. Further, we show that for certain parameter combinations, there may be a potential advantage to slow reporting of test results on the spread of the infection.

3 Method

We developed a deterministic model as a platform of our study. A generic individual is identified in a model compartment based on the disease-specific and test-specific criteria. The former criteria include Susceptible, Infectious and Recovered, thus SIR, and the latter criteria group people in either untested, awaiting for the test result with expectation of positive or negative outcome, or reported positive, thus u, p, n and t, respectively, reflected as subscript. Also, two 'integrator' or 'accumulator' compartments, N and P, were incorporated in the model in order to collect cumulative reported negative or positive tests. The flowchart model is as follows
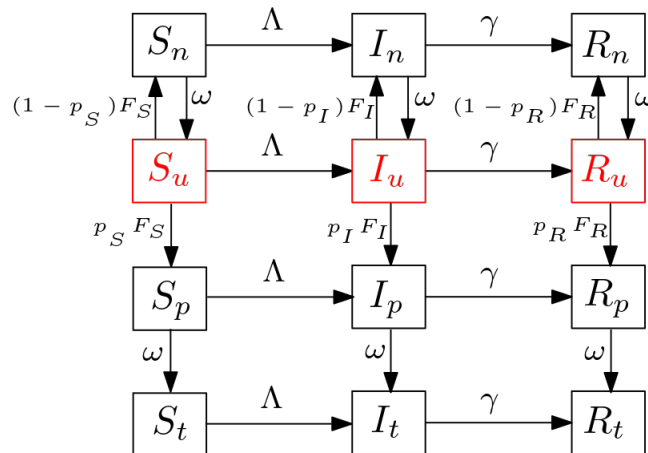

Figure 1: Flowchart of the SIR (Susceptible-Infectious-Recovered) model. [Fady] Say more about the compartments and parameters here to make it stand on its own.

2

The model is

$$dS_u/dt = -\Lambda S_u - F_S S_u + \omega S_n, \tag{1}$$
$$dS_n/dt = -\Lambda S_n + (1 - p_S)F_S S_u - \omega S_n, \tag{2}$$
$$dS_p/dt = -\Lambda S_p + p_S F_S S_u - \omega S_p, \tag{3}$$
$$dS_t/dt = -\Lambda S_t + \omega S_p, \tag{4}$$
$$dI_u/dt = \Lambda S_u - F_I I_u + \omega I_n - \gamma I_u, \tag{5}$$
$$dI_n/dt = \Lambda S_n + (1 - p_I)F_I I_u - \omega I_n - \gamma I_n, \tag{6}$$
$$dI_p/dt = \Lambda S_p + p_I F_I I_u - \omega I_p - \gamma I_p, \tag{7}$$
$$dI_t/dt = \Lambda S_t + \omega I_p - \gamma I_t, \tag{8}$$
$$dR_u/dt = \gamma I_u - F_R R_u + \omega R_n, \tag{9}$$
$$dR_n/dt = \gamma I_n + (1 - p_R)F_R R_u - \omega R_n, \tag{10}$$
$$dR_p/dt = \gamma I_p + p_R F_R R_u - \omega R_p, \tag{11}$$
$$dR_t/dt = \gamma I_t + \omega R_p, \tag{12}$$
$$dN/dt = \omega(S_n + I_n + R_n), \tag{13}$$
$$dP/dt = \omega(I_p + R_p), \tag{14}$$

where β, (in units of 1/day), is the disease transmission rate, η_w and η_t are the isolation parameters for awaiting and reported individuals, respectively. Λ is the force of infection and is defined as

$$\Lambda = \beta \frac{(I_u + \eta_w I_n + \eta_w I_p + \eta_t I_t)}{N_0}, \tag{15}$$

where N_0 is the total population size. Further, ω, (1/day), is the rate of onward flow from the awaiting positive or negative compartments to reported or untested compartments, respectively, γ, (1/day), is the recovery rate, ρ, (1/day), is the per capita testing intensity across the whole population. Further, various testing strategies are incorporated through the compartment-specific relative testing weights W_S, W_I and W_R. What matters in these weight is their relative proportions. For example, $W_I/W_S = 2$ means that, the probability that infected individuals get tested is as twice as that of susceptible individuals. The weighted number of people available for tests is defined as $W = W_S S_u + W_I I_u + W_R R_u$, and the scaling parameter for testing defined as

$$\sigma = \frac{\rho N_0}{W}. \tag{16}$$

Thus, the weighted testing rate is defined as $F_Z = \sigma W_Z$, where $Z \in \{S, I, R\}$. Note that the particular form of σ (16) in the case when no one is left untested, $W \approx 0$, leads to a singularity issue in the simulation. We refer the reader to the Appendix for further details and the solution.

The classical SIR model is based on the following implicit assumptions (see a ref for details); well-mixed population, homogeneity of the population, exponentially distributed duration of infection and large population size (may

3

be refer the reader to Keeling and Rohani (2011)). In addition to these standard assumptions, our model (1) assumes: (i) there is a single force of infection, Λ, that is, where a susceptible individual moves to does not depend on who infected it, (ii) a perfectly specific test, $p_S = 0$, for simplicity in analysis, (iii) $\eta_t \leq \eta_w$, i.e., the individuals awaiting test results have a higher transmission probability than the reported individuals. - [Q] why not birth and death are included? say it or not?

The Disease-Free Equilibrium (Ali, not sure if this is the right term?), DFE hereafter, for the SIR model 1 is given by solving the coupled system including $S_u + S_n = N_0$ and $F_S S_u - \omega S_n = 0$. The DFE is

$$S_n^* = \frac{\rho}{\omega} N_0, \; S_u^* = N_0 - S_n^*, \text{and} I_j = R_j = 0 \text{ for all j.} \tag{17}$$

The Basic reproduction number, $\mathcal{R}_0$, was calculated by using the next generation matrix method developed by Van den Driessche and Watmough (2002). $\mathcal{R}_0$ is

$$\mathcal{R}_0 = (A \times S_u^* + B \times S_n^*) \times C, \tag{18}$$

where

$$A = \gamma(\omega + \gamma) + (\gamma \eta_w + \omega \eta_t p_I) F_I,$$

$$B = \big(\omega + (F_I + \gamma)\eta_w\big)\gamma + \frac{(\eta_w \gamma + \eta_t \omega)\omega p_I F_I}{\omega + \gamma},$$

$$C = \frac{\beta/\gamma}{N_0(\gamma(\omega + \gamma) + F_I(\gamma + \omega p_I))}.$$

Further details are provided in the Appendix.

[to be completed! Something needs to be said here about simulation part]. The analytical calculation of the next generation matrix, G, and the derivation of $\mathcal{R}_0$ was carried out in Maple (ref) by using simple linear Algebra package. We used Ⓡ for the simulation part which included using the explicite expression of $\mathcal{R}_0$ 18 as a function of the underlying parameters, specifying the parameters a realistic range, calculating the corresponding $\mathcal{R}_0$ and plotting the contours of $\mathcal{R}_0$ by using ggplot package in Ⓡ. The related result is presented in Figure 2, where panel (2a) represents the random testing, and panel (2b) is representing non-random testing. The parameter values or ranges are as follows (I like using a table here, with the param, their units and values). It is notable that in the simulation part, the explicit expression of $\mathcal{R}_0$ was used and not the approximation (22). This simulation reflects the behavior of $\mathcal{R}_0$ with respect to the selected parameters for two different testing strategies: (i) random testing, represented by all testing weights to be the same, $W_S = W_I = W_R$, and (ii) non-random testing, when testing weight are not equal. For simmulation purposes we chose $W_S = W_I = W_R = 1$ for random testing, and $W_S = 0.3$ and $W_I = W_R = 1$ for non-random testing strategy. Note that the critical contour of $\mathcal{R}_0 = 1$ is plotted in solid line in Figure 2.

4

4 Results

The explicit formula for the basic reproduction number, $\mathcal{R}_0$ (18), provides an opportunity to study the influence of changes in the underlying parameters on the critical index of epidemic dynamics. We are interested in understanding the effect of parameters that can be realistically controlled by changing in isolation, testing intensity and test resulting, i.e., η_t and η_w, ρ and ω, respectively. The following Proposition is the direct result of taking partial derivative of $\mathcal{R}_0$ (18) with respect to selected parameters.

Proposition 1. Using the expression of $\mathcal{R}_0$ (18),

1. $\partial R_0/\partial \eta_t \geq 0$ and $\partial R_0/\partial \eta_w \geq 0$.

2. $\partial \mathcal{R}_0/\partial \rho \leq 0$ when $\rho \approx 0$.

3. $\partial R_0/\partial \omega$ can be positive or negative when $\rho \approx 0$.

Given that the perfect isolation occurs at $\eta_t = \eta_w = 0$, Prop. 1 means that lifting the isolation from awaiting group results in an increased $\mathcal{R}_0$ and consequently a greater number of infected individuals. We used Taylor approximation of $\mathcal{R}_0$ at $\rho = 0$ due to the complexity of the expression and thus inconclusive. See the Appendix for details. It is straightforward to derive 2 and 3 from the linear approximation of $\mathcal{R}_0$ at $\rho = 0$.

Prop. 2 indicates that increasing testing intensity reduces the $\mathcal{R}_0$. This is sensible since as people are moved to test compartments (I_p, I_n ⟨**Fady:** *the susceptibles also reduce contact and transmission* ⟩) the higher probability of being subject to isolation and the lower the transmission (15) will become.

Of these results, prop. 3 is the most surprising. It states that returning test results more rapidly (i.e., increasing ω) does not necessarily lower $\mathcal{R}_0$, rather, whether increasing ω lowers $\mathcal{R}_0$ is dependant on the precise combination of model parameters (test reporting rate itself, testing processes/strategies (W's), testing efficacy (P_I) and isolation (η's). Specifically, the $\partial R_0/\partial \omega > 0$ suggests that reproduction number may increase as the test reporting proccess become faster. This can be seen from expression (23) in the case of "perfect isolation", when $\eta_w = 0$ and $\eta_t = 0$. The underlying mechanism for this result is that individuals may take more precautionary behaviours (e.g., physical distancing) when they are awaiting test results compared to when they are untested or their test has returned negative. An example of a situation that would favour slow return of tests is if the test being employed produces many false negatives, because many infected individuals will believe they are negative and thus may unknowingly spread the virus to many others. For an example of the behaviour of $\mathcal{R}_0$ see Figure 2 at varying values of ω. This property also provides a tool to quantify the amount of delay required in the test reporting process as a strategy to reduce $\mathcal{R}_0$ and consequently control the epidemic.

[comments about the figure:] 1- use a single legend, change the range manually.
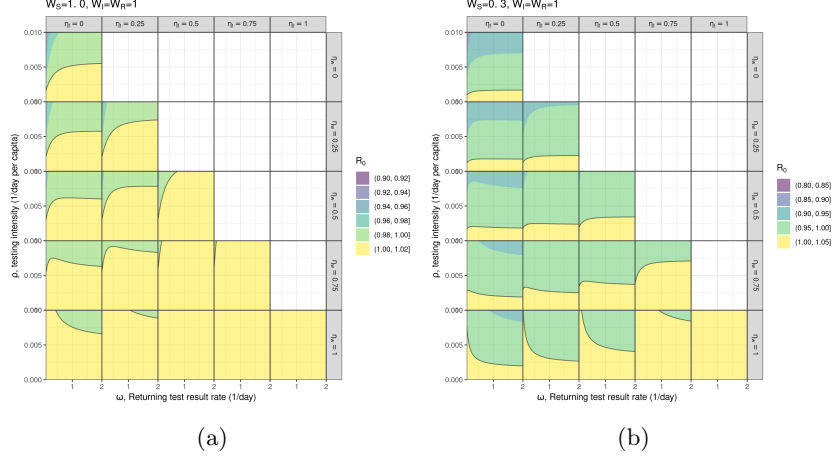
Figure 2: Behaviour of the basic reproduction number, $\mathcal{R}_0$, with respect to changes in the underlying parameters; remind the reader about the parameters and their values in this simulations. the solid line in each panel represents the critical contour of $\mathcal{R}_0 = 1$.

Our numerical simulation in support of the analytical results in Proposition 1 are presented in Figure 2. It can be infered that when random testing strategy is applied, Figure 2a, comparing to the non-random testing strategy, Figure 2a, the critical testing intensity of the coresponding panels are lower in non-random testing. Also, it appears that speeding the test reporting, i.e., increasing ω, does not significantly lower $\mathcal{R}_0$ when awaiting people follow the isolation perfectly, i.e., η_w is closer to 0. However, speeding the test reporting reduces the epidemy more when the awaiting people less follow the isolation, i.e., η_w is closer to 1.

Furthermore, we derived an inequality that quantifies the exact relationships between model parameters that result in returning tests more rapidly being favorable (29). To give a biological interpretation, we describe the qualitative *trends* predicted by the inequality. Returning test results more rapidly *tends* to be more favorable when

- individuals who have tested positive lower their contact much more than individuals who are waiting for their test results (i.e., $\eta_t \ll \eta_w$).

- the test is sensitive.

- testing of infected individuals is more intense than testing of susceptible individuals.

An in-depth discussion of these results is presented in the discussion section.

The use of tests cheaper than RT-PCR has been proposed as a potential strategy for containing the COVID-19 pandemic. While cheaper tests may be less sensitive and reliable than RT-PCR, they allow for broader and more intense

testing. Using our Taylor approximation of $\mathcal{R}_0$ near $\rho = 0$, we examined what circumstances (i.e., model parameters) make the use of one test more favourable than another, and give a complete description through inequality 30. In general, we found that the expensive test *tends* to more effectively lower $\mathcal{R}_0$ when

- individuals who test positive self-isolate much more than individuals who are waiting for their test result.

- the time it takes to return tests is much shorter than the mean infectious period.

- the testing intensity is much greater for infected individuals than susceptible individuals.

Our model also predicts an asymmetry between cheap and expensive tests: if a cheap test can identify on average more infected individuals as an expensive test, then our model predicts that the cheap test will lower $\mathcal{R}_0$ more. In contrast, if an expensive test can identify on average more infected individuals, it will not necessarily lower $\mathcal{R}_0$ more than the cheap test. ⟨**Fady:** *we can state this as a formal proposition in equations rather than in words, if that would be better.* ⟩

5   Discussion

- JD's email: We're basically looking at the potential advantage of slow tests: people waiting for test results may be more careful than those who have received negatives. These advantages are real, and neglected. We also compare to an individual-level advantage of fast tests: people who test positive may be even more careful. But we are missing out on community-level advantages of fast testing: better assessment of the situation, identification of hot spots, contact-tracing, etc.

- May be something about the testing rate/intensity, now the per capita testing intensity is very low ($\rho \approx 0$). In near future new test kits may be widely accessible, our model provide insights in this case (what are those?)

- "delay negative results" result

5.1   Rate of returning tests

Our model predicts that when the difference in self-isolation between individuals waiting for their tests and individuals who are confirmed positive is small, returning tests rapidly is not beneficial. The underlying mechanism for this prediction is that the benefit in returning tests rapidly so (i.e., the extra self-isolation an individual does when they test positive) is minimal and outweighed by the fact that those who test negative may increase their contacts. Thus, in such a case, returning tests more rapidly is expected to increase $\mathcal{R}_0$. Similarly, if the test is not sensitive, many infected individuals will test negative, and

thus may increase their contacts under the false belief that they are not infectious, so returning tests rapidly in this case may also contribute to increased transmission.

When testing of infected individuals is more intense than susceptible individuals, returning test results rapidly is beneficial because those infected individuals will be informed and self-isolate. Conversely, if testing of susceptible individuals is much greater, very few tests will be positive, and the benefit of informing those few positive cases will be outweighed by the potential increase in contacts of the individuals testing negative.

5.2 Expensive vs. cheap tests

⟨**Fady:** *I think we should discuss this before I write it. I'm a little hesitant to really expand on these results because of the points JD brought up over email.*⟩

References

Arino, J. and Portet, S. (2020). A simple model for COVID-19. *Infectious Disease Modelling*.

Bergstrom, T., Bergstrom, C. T., and Li, H. (2020). Frequency and accuracy of proactive testing for COVID-19. *medRxiv*.

de Celles, M. D., Casalegno, J.-S., Lina, B., and Opatowski, L. (2020). Influenza may facilitate the spread of SARS-CoV-2. *medRxiv*.

Elbanna, A., Wong, G. N., Weiner, Z. J., Wang, T., Zhang, H., Liu, Z., Tkachenko, A. V., Maslov, S., and Goldenfeld, N. (2020). Entry screening and multi-layer mitigation of COVID-19 cases for a safe university reopening. *medRxiv*.

Endo, A., Leclerc, Q. J., Knight, G. M., Medley, G. F., Atkins, K. E., Funk, S., Kucharski, A. J., et al. (2020). Implication of backward contact tracing in the presence of overdispersed transmission in COVID-19 outbreaks. *Wellcome Open Research*, 5(239):239.

Jenness, S. M., Willebrand, K. S., Malik, A. A., Lopman, B. A., and Omer, S. B. (2020). Modeling dynamic network strategies for SARS-CoV-2 control on a cruise ship. *medRxiv*.

Keeling, M. J. and Rohani, P. (2011). *Modeling infectious diseases in humans and animals*. Princeton University Press.

Larremore, D. B., Wilder, B., Lester, E., Shehata, S., Burke, J. M., Hay, J. A., Tambe, M., Mina, M. J., and Parker, R. (2020). Test sensitivity is secondary to frequency and turnaround time for COVID-19 surveillance. *MedRxiv*.

Lopman, B., Liu, C., Le Guillou, A., Handel, A., Lash, T. L., Isakov, A., and Jenness, S. (2020). A model of COVID-19 transmission and control on university campuses. *medRxiv*.

Rice, K., Wynne, B., Martin, V., and Ackland, G. J. (2020). Effect of school closures on mortality from coronavirus disease 2019: old and new predictions. *BMJ*, 371.

Ross, R. (1911). *The prevention of malaria*. John Murray.

Ruszkiewicz, D. M., Sanders, D., O'Brien, R., Hempel, F., Reed, M. J., Riepe, A. C., Bailie, K., Brodrick, E., Darnley, K., Ellerkmann, R., et al. (2020). Diagnosis of COVID-19 by analysis of breath with gas chromatography-ion mobility spectrometry: a feasibility study. *EClinicalMedicine*, page 100609.

Tuite, A. R., Fisman, D. N., and Greer, A. L. (2020). Mathematical modelling of COVID-19 transmission and mitigation strategies in the population of Ontario, Canada. *CMAJ*, 192(19):E497–E505.

Van den Driessche, P. and Watmough, J. (2002). Reproduction numbers and sub-threshold endemic equilibria for compartmental models of disease transmission. *Mathematical biosciences*, 180(1-2):29–48.

6 supplementary material

6.1 Calculation of $\mathcal{R}_0$

The next generation matrix is $G = FV^{-1}$, where matrix F represents the inflow of new infection to the infected compartments and matrix V represents the flow in the infected compartments when the population is totally susiptable. For model (1), F and V are

$$F = \beta/N_0 \begin{bmatrix} S_u & \eta_w\, S_u & \eta_w\, S_u & \eta_t\, S_u \\ S_n & \eta_w\, S_n & \eta_w\, S_n & \eta_t\, S_n \\ 0 & 0 & 0 & 0 \\ 0 & 0 & 0 & 0 \end{bmatrix}, \tag{19}$$

$$V = \begin{bmatrix} F_I + \gamma & -\omega & 0 & 0 \\ -(1-p_I)F_I & \omega + \gamma & 0 & 0 \\ -p_I F_I & 0 & \omega + \gamma & 0 \\ 0 & 0 & -\omega & \gamma \end{bmatrix}. \tag{20}$$

The particular form of F with two rows of zeros at the bottom, simplifies G as

$$G = \begin{bmatrix} G_{11} & G_{12} \\ 0 & 0 \end{bmatrix}, \text{ where } G_{11} = C \begin{bmatrix} A\, S_u & B\, S_u \\ A\, S_n & B\, S_n \end{bmatrix}. \tag{21}$$

Note that the block matrix G_{12} does not influence $\mathcal{R}_0$ defined as the spectral radius of G. All matters here are the eigenvalues of G_{11}, which are 0 and $\mathcal{R}_0$ (18).

6.2   On Testing Rate and Numerical Singularity

The testing rate, σ, should be formulated such that people from the untested compartments will not be tested if they are not there. The numerical singularity issue with the chosen σ (16) is that the population in S compartments appeared to blow up when the DFE is achieved. This is once the only untested people are susceptibles, the FOI will become $\Lambda = 0$, testing rate $F_s = \rho N_0/S_u$. Thus, eq(1) of the model will be $dS_u/dt = -\rho N_0 + \omega S_n$ which is no longer dependent on S_u and a linear rate of leaving the S_u compartment.

One way to fix this issue, is to consider a maximum testing rate, τ (1/day). In general, we want to test at a rate of ρ across the whole population. This won't always be possible, so we impose a maximum rate of τ per testable person and redefine $\sigma = \frac{\tau \rho N_0}{\tau W + \rho N_0}$, with the assumption that $\tau \gg \rho$. This alteration in σ, does not change any results related to $\mathcal{R}_0$, thus we only impose it in the simulation of the epidemic dynamic.

6.3   Taylor Approximation of $\mathcal{R}_0$ at $\rho = 0$

The basic reproduction number, $\mathcal{R}_0$, close to $\rho = 0$ can be approximated linearly in ρ by using Taylor approximation. it follows

$$R_0 \approx \beta/\gamma + \frac{\beta\rho}{\omega(\omega+\gamma)\gamma^2 W_S} \Big(\gamma(\eta_w - 1)(\gamma W_S + \omega W_I) + (\eta_t - 1)P_i W_i \omega^2 \Big) + \mathcal{O}(\rho^2).$$
(22)

Also, to analyze the influence of ω on $\mathcal{R}_0$, the approximation (22) was used. Then it is straight forward to have

$$\partial R_0/\partial \omega = \frac{-\beta\rho}{\gamma W_S \omega^2 (\gamma+\omega)^2}(a\omega^2 + b\omega + c),$$
(23)

where $a = (\eta_w - 1)W_I - (\eta_t - 1)P_I W_I = ((s - p_I)\eta_t + (p_I - 1))W_I$, $b = 2(\eta_w - 1)\gamma W_S$ and $c = (\eta_w - 1)\gamma^2 W_S$. Given that $0 \le \eta_t \le \eta_w \le 1$, one can easily derive $b \le 0$ and $c \le 0$.

Note that in general, the necessary and sufficient condition for $a \ge 0$ is $(s - p_I)\eta_t \ge (1 - p_I)$, where $s = \frac{\eta_w}{\eta_t} \ge 1$.

Note that in case of "perfect isolation", i.e., when $\eta_w = 0$ and consequently $\eta_t = 0$, it is straight forward to see that $a \le 0$, $b < 0$ and $c < 0$. Thus, $\partial \mathcal{R}_0/\partial \omega \ge 0$. As an example, in the case of a very accurate testing regime, i.e., $P_I = 1$, $a \ge 0$ is achieved. If $a \ge 0$, the quadratic expression in (23), has Real roots. Assuming that $\omega_1 < 0$ and $\omega_2 > 0$ be the roots of the quadratic expression in $\partial R_0/\partial \omega$. Thus, $\partial R_0/\partial \omega > 0$ for $0 < \omega < \omega_2$ and $\partial R_0/\partial \omega < 0$ for $\omega > \omega_2$.

[Fady: this subsection and most of the next belong to the Appendix since they are very detailed. Would you clean up the writing, there are some repeated expressions that can be referenced?]

6.4   rate of returning tests

The linearization of $\mathcal{R}_0$ around $\rho = 0$ is

$$\mathcal{R}_0 \approx \beta/\gamma + \frac{\beta\rho}{\omega(\omega+\gamma)\gamma^2 W_s}\Big(\gamma(\eta_w - 1)(\gamma W_s + \omega W_i) + (\eta_t - 1)P_i W_i \omega^2\Big). \quad (24)$$

So when $\rho \approx 0$ we have

$$\partial \mathcal{R}_0/\partial \omega \approx \frac{-\beta\rho}{\gamma W_s \omega^2 (\gamma+\omega)^2}(a\omega^2 + b\omega + c).$$

where $a = (\eta_w - 1)W_i - (\eta_t - 1)P_i W_i$, $b = 2(\eta_w - 1)\gamma W_s$ and $c = (\eta_w - 1)\gamma^2 W_s$.

Perhaps counter-intuitively, the equation above does not predict that $\mathcal{R}_0$ is monotone decreasing with respect to ω. In other words; our model does not predict that returning test results more rapidly *always* lower $\mathcal{R}_0$. In order to gain insight into this intriguing behavior, we examine the zeroes of $\frac{\partial \mathcal{R}_0}{\partial \omega}(\omega)$.

Defining the following quantity, Q, will help us write the roots of $\partial \mathcal{R}_0/\partial \omega$ neatly.

$$Q = \frac{W_i}{W_s}\left(1 - \frac{n_t - 1}{n_w - 1}P_i\right) \quad (25)$$

$$(26)$$

With that in mind, we can write the roots of $\partial \mathcal{R}_0/\partial \omega$ as

$$\omega_1 = \frac{\gamma}{-\sqrt{1-Q}-1} \quad (27)$$

$$\omega_2 = \frac{\gamma}{\sqrt{1-Q}-1} \quad (28)$$

Note that the zeroes are real if and only if $Q < 1$. Note that have $\eta_t < \eta_w$, so if $P_i \approx 1$, we will have $Q < 0 < 1$. Thus, if we assume near-perfect test sensitivity, ω_1 and ω_2 will be real.

Assuming ω_1, ω_2 are real, it is easy to confirm that $\omega_1 < 0$ by looking at the denominator. To see that $\omega_2 > 0$, recall that $Q < 0$, so $\sqrt{1-Q} > 1$ and so $\sqrt{1-Q}-1 > 0$. Knowing that $\omega_1 < 0$, the only root of interest (i.e., biologically relevant quantity) is ω_2.

We can prove that $\partial \mathcal{R}_0/\partial \omega > 0$ when $\omega \in (0, \omega_2)$ and $\partial \mathcal{R}_0/\partial \omega < 0$ when $\omega \in (\omega_2, \infty)$ by computing the limits of $\partial \mathcal{R}_0/\partial \omega$ at 0 and ∞ respectively. So it follows that $\mathcal{R}_0$ has a global maximum with respect to ω at $\omega = \omega_2$.

Now we want to characterize the parameter regions on which $\partial \mathcal{R}_0/\partial \omega < 0$ (i.e., the conditions under which returning test results more rapidly is favorable). By the previous analysis, this is equivalent to solving for $\omega > \omega_2$. So

$$\omega > \omega_2$$

$$\omega > \frac{\gamma}{\sqrt{1-Q}-1}$$

$$\vdots$$

$$\frac{1-n_t}{1-n_w}P_i > \frac{W_s}{W_i}\left(\frac{\gamma}{\omega}+1\right)^2 \tag{29}$$

6.5 Expensive vs. cheap tests

The use of tests cheaper than RT-PCR has been proposed as a potential strategy for containing the COVID-19 pandemic. While cheaper tests may be less sensitive and reliable than RT-PCR, they allow for broader and more intense testing. In the analysis below, we compare the $\mathcal{R}_0$ predicted by our model depending on the testing strategy.

Consider a test that allows us to test at rate ρ_1 and has sensitivity $P_{i,1}$, and another test that allows us to test at ρ_2 and has sensitivity $P_{i,2}$. Suppose that $\rho_1 > \rho_2$. Recall that the linearization of $\mathcal{R}_0$ around $\rho \approx 0$ is given by

$$\mathcal{R}_0 \approx \beta/\gamma + \frac{\beta\rho}{\omega(\omega+\gamma)\gamma^2 W_s}\Big(\gamma(\eta_w-1)(\gamma W_s+\omega W_i)+(\eta_t-1)P_i W_i\omega^2\Big).$$

Treating $\mathcal{R}_0$ as a function of ρ and P_i, we can reduce the inequality

$$\mathcal{R}_0(\rho_2,P_{i,2}) < \mathcal{R}_0(\rho_1,P_{i,1})$$

into

$$\rho_1\left(\gamma(\eta_w-1)(\gamma W_s+\omega W_i)+(\eta_t-1)P_{i,1}W_i\omega^2\right)-\rho_2\left(\gamma(\eta_w-1)(\gamma W_s+\omega W_i)+(\eta_t-1)P_{i,2}W_i\omega^2\right) > 0$$

$$\vdots$$

$$\frac{\rho_2 P_{i,2}-\rho_1 P_{i,1}}{\rho_1-\rho_2} > \frac{1-\eta_w}{1-\eta_t}\cdot\frac{\gamma(\gamma W_s+\omega W_i)}{\omega^2 W_i} \tag{30}$$

Note that the RHS is positive, thus a necessary condition for the inequality above to hold is that $\rho_2 P_{i,2} > \rho_1 P_{i,1}$, equivalently

$$\frac{P_{i,2}}{P_{i,1}} > \frac{\rho_1}{\rho_2}. \tag{31}$$

To state an example of this, if test A is three times as expensive as test B (and hence one can test three times as many people with test B), using test A rather than B will be favorable only if test A is at least 3 times more sensitive than test B. Note that this is a necessary but not sufficient condition, so even if test A is three times more sensitive, it is still possible for test B to be more effective.

12

Eq. (30) tells us precisely when a test corresponding to $\rho_2, P_{i,2}$ will yield a lower $\mathcal{R}_0$ than a test corresponding to $\rho_1, P_{i,1}$, where $\rho_1 > \rho_2$. Some of the qualitative *trends* that favor test 2 (the higher-sensitivity test) include

- individuals who test positive self-isolate much more than individuals who are waiting for their test result.

- the time it takes to return tests is much shorter than the mean infectious period.

- the testing intensity is much greater for infected individuals than susceptible individuals.

6.6 Literature Review

6.6.1 Explicit models of TTI (trace/test/isolate) based on network or agent-based models

(Endo et al., 2020) [Ali: It seems to me that this is just a statistical model to estimate the parent-offspring of an infected index, not sure if it fits into agent-based group!] Used simulation on a branching process model to assess the forward and backward contact tracing efficiency. Assuming a negative-binomial branching process with a mean R, reproduction number, and overdispersion parameter k, the mean total number of generation G3 and averted G3 are estimated. The effectiveness of TTI is defined as the ratio of averted to the mean.

(Jenness et al., 2020) developed a network-based transmission model for SARS-CoV-2 on the Diamond Princess outbreak to characterize transmission dynamics and to estimate the epidemiological impact of outbreak control and prevention measures.

(Elbanna et al., 2020) [seems similar to MacPan model!]

(de Celles et al., 2020) Was discussed in the Math 747 SEIR Asymptomatic and symptomatic I_1, I_2. Used linear chain trick Stringency index as a control force lowering β.

(Rice et al., 2020) Effect of school closures on mortality. Reproduce Report 9 results by spatial agent based CovidSim.

6.6.2 Models of repeated random testing of isolated populations

Bergstrom et al. (2020) (1) Model, assumptions: They developed a function, namely expected exposure $E(C, \tau)$, to approximate trade-offs between the frequency of testing, n, the sensitivity of testing, q, and the delay between testing and results, d. This function is explicitly derived and was connected the effective reproduction number $R = R_0 S$, where S is the proportion of population susceptible. assumption that transmission rates are a step function: individuals who have COVID go from non-infectious to fully infectious instantaneously, and remain fully infectious until they are no longer able to transmit disease. Test sensitivity takes the same form over the course of infection. More sophisticated

models could allow varying infectiousness and varying sensitivity over time, as in (Larremore et al., 2020).

(Lopman et al., 2020) Used a Deterministic SEIR model, incorporated TTI, applicable to a university setting. They assumed a fairly high reproductive number that is not reduced through social distancing measures. They found that community-introduction of SARS-CoV-2 infection onto campus can be relatively controlled with effective testing, isolation, contract tracing and quarantine.

(Tuite et al., 2020) used an age-structured compartmental model of COVID-19 transmission in the population of Ontario, Canada. We compared a base case with limited testing, isolation and quarantine to different scenarios.

6.6.3 Other maybe-related works

(Arino and Portet, 2020) developed a SLIAR compartmental model to study the spread of an epidemic, specifically COVID-19, in a population. The model incorporates an Erlang distribution of times of sojourn in incubating, symptomatically and asymptomatically infectious compartments. Basic reproduction number is derived. Also, sensitivity analysis with respect to the underlying parameters for the following two outputs was carried out; (i) the number of observable cases during the course of the epidemic and at the peak, and (ii) the timing of the peak of the outbreak. Sensitivity analysis is performed using the R package multisensi.

(Ruszkiewicz et al., 2020) novel with-in-a-minute breath testing with 80% accuracy.